Food Chemistry: X 12 (2021) 100143

Contents lists available at ScienceDirect

Food Chemistry: X

journal homepage: www.sciencedirect.com/journal/food-chemistry-x

Chemical characterization of flavonoids and alkaloids in safflower (*Carthamus tinctorius* L.) by comprehensive two-dimensional hydrophilic interaction chromatography coupled with hybrid linear ion trap Orbitrap mass spectrometry

Songsong Wang [a,1], Jiliang Cao [b,1], Jiagang Deng [c], Xiaotao Hou [c], Erwei Hao [c], Lei Zhang [d], Hua Yu [a,*], Peng Li [a,*]

[a] State Key Laboratory of Quality Research in Chinese Medicine, Institute of Chinese Medical Sciences, University of Macau, Macao 999078, China
[b] College of Pharmacy, Shenzhen Technology University, Shenzhen 518118, China
[c] Collaborative Innovation Center of Research on Functional Ingredients from Agricultural Residues, Guangxi Key Laboratory of Efficacy Study on Chinese Materia Medica, Guangxi University of Chinese Medicine, Nanning 530200, China
[d] Laboratory Animal Center, Sichuan Academy of Chinese Medicine Sciences, Chengdu 610041, China

ARTICLE INFO

Keywords:
Online HILIC×HILIC
LTQ-Orbitrap mass spectrometry
Flavonoids
Alkaloids
Carthamus tinctorius L

ABSTRACT

Safflower (*Carthamus tinctorius* L.) is a famous food additive and herbal medicine in China. In the present research, an online comprehensive two-dimensional hydrophilic interaction chromatography coupled to a diode array detector and a hybrid linear ion trap-Orbitrap mass spectrometry (HILIC × HILIC-DAD-ESI/HRMS/MS^n) platform was developed to analyze the flavonoids and alkaloids in safflower. By combining with an XBridge Amide column (150 mm × 4.6 mm, 3.5 μm) and an Ultimate amide column (50 mm × 4.6 mm, 5 μm), the system orthogonality reached 88% and a total of 231 peaks were detected. Altogether 93 compounds, including 75 flavonoids and their glycosides and 10 alkaloids were unambiguously or tentatively identified in both negative and positive ion modes, using accurate mass and MS fragment data. Among them, 5 compounds were discovered and reported from safflower for the first time. The established HILIC × HILIC platform should be a powerful tool for the separation and characterization of complicated matrices in natural herbs.

Introduction

Recently, two-dimensional liquid chromatography (2D-LC) has been widely applied to the separation and analyses of complicated samples due to its excellent separation capability, high resolution, and large peak capacity (Liang et al., 2012; Paola Dugo et al., 2004). The elution from the first dimension (^{1}D) can be collected as fractions that will be individually transferred and separated in the second dimension (^{2}D), providing a feasible tool for separation, identification, and quality control of complex chemicals (Donato et al., 2011; Wang et al., 2008). To achieve high orthogonality, the two dimensions usually employ columns with different separation mechanisms, for example, reversed-phase (RP), normal phase (NP), hydrophilic interaction liquid chromatography (HILIC), size exclusion chromatography (SEC), affinity chromatography (AC), or ion-exchange chromatography (IEX), presenting different selectivities (Li et al., 2014; Li et al., 2015; Sommella et al., 2017; Uliyanchenko et al., 2012). Once coupled to mass spectrometry (MS), 2D-LC can be a more powerful platform with unparalleled capability for chemical separation and identification in samples with complex matrices.

Safflower (*Carthamus tinctorius* L.), known as Honghua in China, is a famous natural pigment, food additive, and cosmetic (Dai et al., 2014). Red and yellow pigments (e.g. carthamin) can be found in the petals of safflower, and are usually applied to dyeing agents in textile and food industries. Also, safflower is considered an emergent oilseed crop (Villa et al., 2017). Moreover, safflower is a popular herbal medicine widely applied for the treatment of coronary heart disease, stroke, and angina pectoris (Delshad,et al., 2018). Nowadays, several derived products are

* Corresponding authors.
E-mail addresses: bcalecyu@um.edu.mo (H. Yu), pengli@um.edu.mo (P. Li).
[1] These authors contributed equally to this work.

https://doi.org/10.1016/j.fochx.2021.100143
Received 28 July 2021; Received in revised form 12 October 2021; Accepted 14 October 2021
Available online 16 October 2021

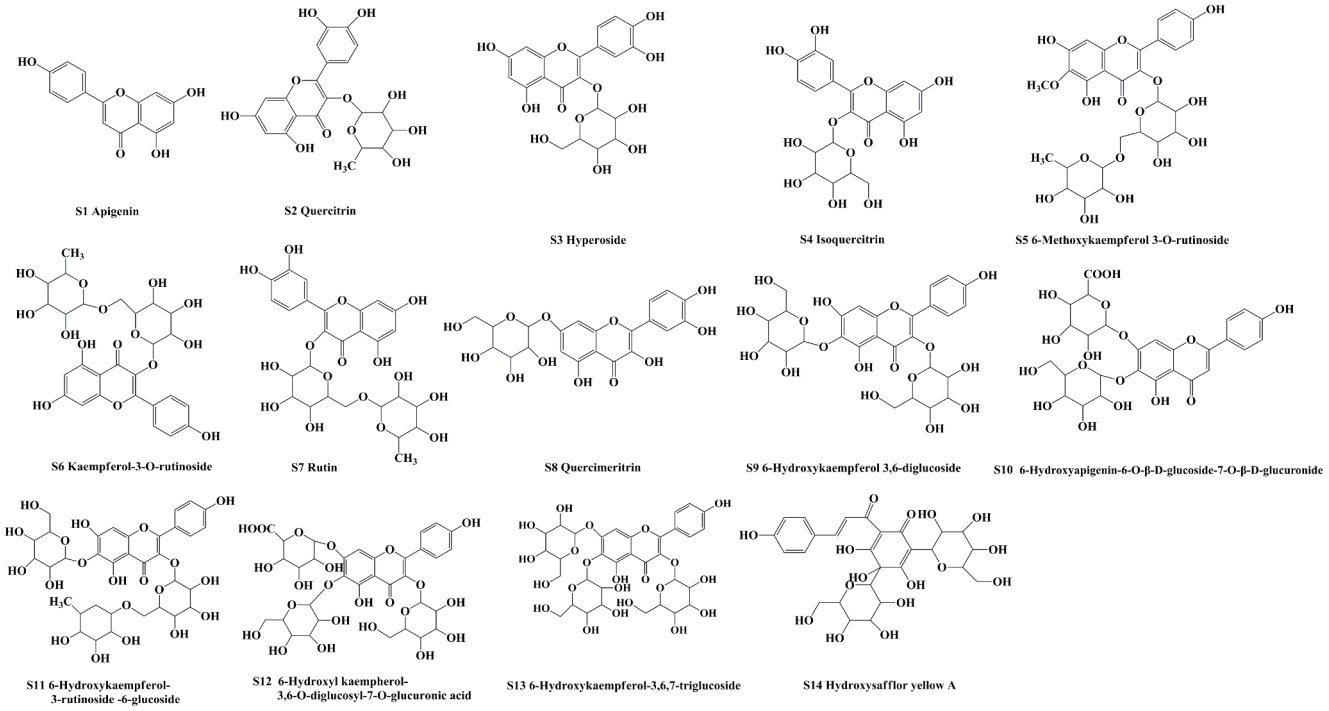

Fig. 1. The chemical structures of the 14 reference compounds.

used to treat cardiovascular and cerebrovascular diseases (Cao et al., 2014; He et al., 2012). Therefore, to scientifically assess the quality of safflower and related products, it is necessary to uncover its chemical compositions, especially the potential bioactive compounds. Flavonoids and their glycosides (O- and C-glycosides) are a group of vital phytochemicals that are related to the therapeutic effects of safflower as a result of their diverse bioactivity (Xiao et al., 2016; Zhang et al., 2016). In addition, alkaloids are active ingredients widely present in safflower and have shown antioxidant, neuroprotective, and hepatoprotective activities both *in vitro* and *in vivo* (Zhang et al., 2016).

In most previous studies, the identification of chemical compounds in safflower was mainly based on one-dimensional LC (1D-LC) or offline 2D-LC/MS analyses (Lu et al., 2019; Yao et al., 2017). Although large number of compounds were characterized in the offline 2D-LC/MS analyses, time consumption and sample loss are the biggest concerns. To our knowledge, no reports about the online HILIC × HILIC 2D-LC systems were recorded for the chemical analysis of safflower. Our research group has developed online 2D-LC (HILIC × RP and RP × RP) systems to characterize diterpenoids and phenolic compounds in *Salvia Miltiorrhiza*, exhibiting remarkable separation power for complex samples (Cao et al., 2017; Cao et al., 2016). Therefore, in the present work, we developed an online comprehensive HILIC × HILIC system coupled with DAD detector and hybrid linear ion trap (LTQ)-Orbitrap mass spectrometry (HILIC × HILIC-DAD-ESI/HRMS/MS^n) to systematically analyze the chemical constituents from safflower. The established HILIC × HILIC system showed good orthogonality and peak capacity, and no solvent effect occurred. Besides, chemical components including flavonoid C- and O-glycosides and alkaloids were characterized. This work will generate crucial knowledge for developing HILIC × HILIC system to analyze natural products with complex compounds.

Materials and methods

Chemicals and materials

Methanol, formic acid, and LC-grade acetonitrile were provided by Merck (Darmstadt, Germany). A Milli-Q purification system (Millipore, Bedford, MA, USA) was used to produce deionized water. Chemical reference standards, including quercetin (>98%), rutin (>98%), hyperoside (>98%), isoquercitrin (>98%), hydroxysafflor yellow A (>98%), kaempferol (>98%), myricetin (>96%), nicotiflorin (>96%), quercimeritrin (>98%), 6-methoxykaempferol-3-O-rutinoside (>96%), luteolin (>98%), apigenin (>98%), 6-hydroxykaempferol-3,6-diglucoside (>98%),6-hydroxykaempferol-3,6,7-triglucoside (>98%), and baicalin (>96%) were provided by Nanjing Jingzhu Bio-Tech Co., Ltd (Nanjing, China), and their chemical structures are shown in Fig. 1. Before use, all reference standards were determined by HPLC-DAD-HRMS/MS^n and confirmed with UV spectra, accurate mass, and MS^n data. Raw samples of Safflower were provided by Tong Ren Tang of Beijing (Macau, China). The voucher specimens were preserved in the Institute of Chinese Medical Sciences, University of Macau, Macao.

Sample preparation and standard solutions

The safflower samples were dried with air circulation at room temperature. The safflower samples were extracted following previous reported methods with minor modifications (Wang et al., 2015). An aliquot of 1 g sample powder was accurately weighed and extracted with 8 mL of 25% ethanol (*v/v*) by an ultrasonic cleaner (44 kHz, Branson Ultrasonic Corp., Danbury, CT, USA) at around 25 °C for 15 min. After centrifugation at 3,000 × *g* for 10 min, the supernatant was filtered through a 0.22 μm membrane (PVDF Millex-GV, 13 mm, Millipore) before 2D-LC analysis.

Next, 25% ethanol (*v/v*) was used to the dissolve the reference standards to obtain individual stock standard solutions with concentrations ranging from 0.8 to 3.2 mg/mL. Appropriate amounts of the individual stock solutions were mixed to obtain a mixed standard solution and then diluted to about 20 μg/mL.

Online HILIC × HILIC-DAD-ESI/HRMS/MS^n analyses

A Dionex UltiMate 3000 × 2 Dual RSLC system (Dionex, Thermo Fisher Scientific Inc., USA) was used for HILIC × HILIC analyses, including a WPS-3000TRS autosampler, an SRD-3600 degasser, a DGP-

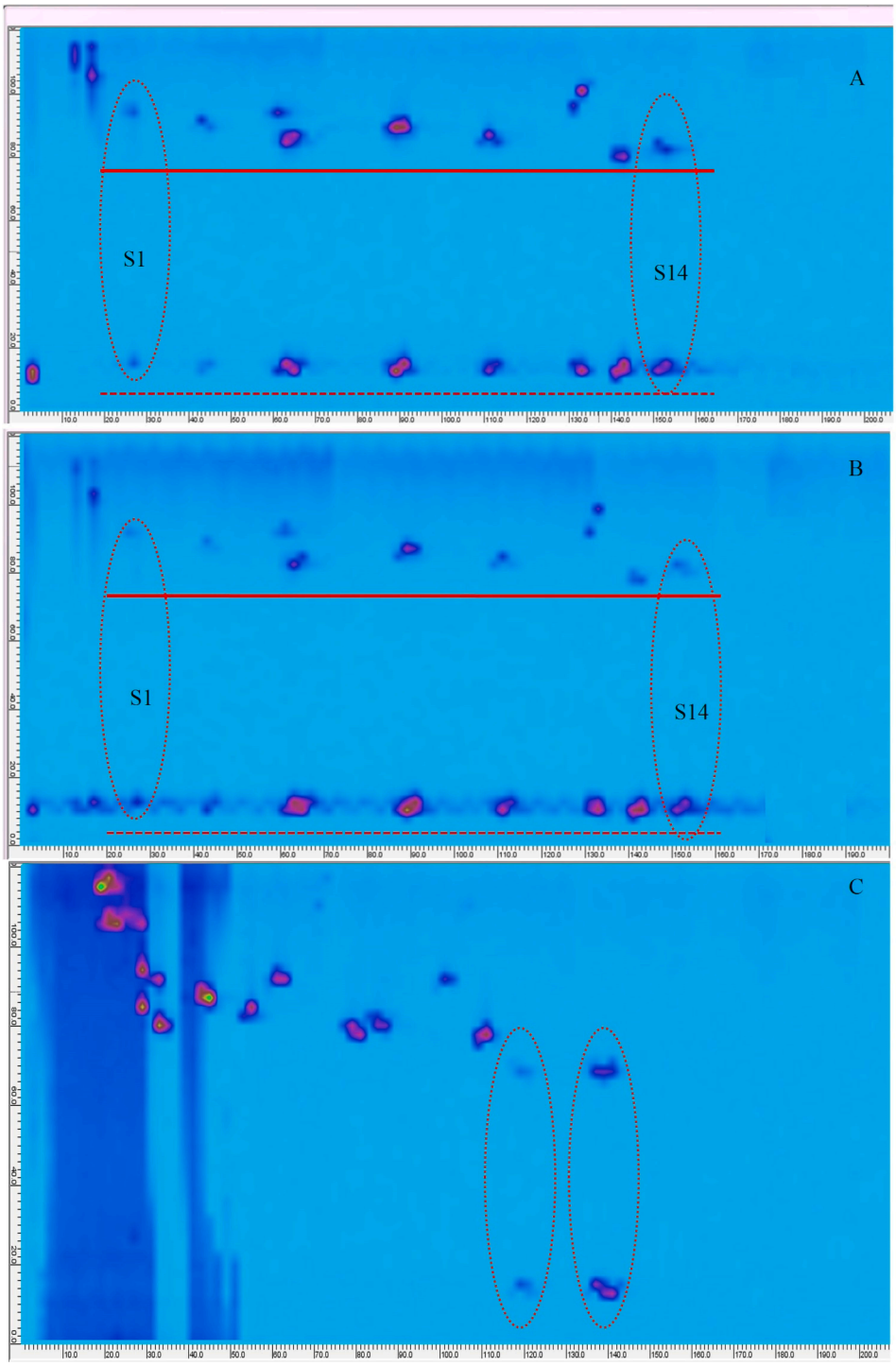

Fig. 2. 2D-TIC contour plots of different 2D-LC systems for separation of 14 reference compounds standards. (A) Combination of HILIC with Hypersil gold PFP column, (B) Combination of HILIC with Accucore Polar Premium column, (C) Combination of HILIC with Accucore Polar Premium column configured with online dilution module.

3600RS dual-ternary pump (right and left pump), a TCC-3000RS column thermostat, and a DAD-3000RS detector. An electronically controlled two-position ten-port switching valve equipped with two sample loops (200 μL, Rheodyne, CA, USA) was configured to connect the ^{1}D and ^{2}D. The 2D-LC system was connected to a hybrid LTQ-Orbitrap XL mass spectrometry (Thermo Fisher Scientific, Bremen, Germany) equipped with electrospray ionization (ESI) source by a flow splitter (Analytical Scientific Instruments, CA, USA) using a fixed ratio at 1:4. The online HILIC × HILIC-LTQ-Orbitrap platform was controlled by the Xcalibur 2.1 software (Thermo Fisher Scientific, Bremen, Germany).

In the ^{1}D separation, the column flow rate (XBridge Amide column, 150 mm × 4.6 mm, 3.5 μm, Waters) was 0.08 mL/min. The mobile phases were 0.1% aqueous formic acid (*v*/*v*) solution (A) and acetonitrile (B). The following gradient program was employed: 0 min, 95% B; 10 min, 95% B; 20 min, 92% B; 30 min, 92% B; 140 min, 82% B; 150 min, 60% B; 172 min, 50% B.

In the ^{2}D separation, a high flow rate of 3 mL/min was applied to the short ^{2}D column (Ultimate amide column, 50 mm × 4.6 mm, 5 μm,

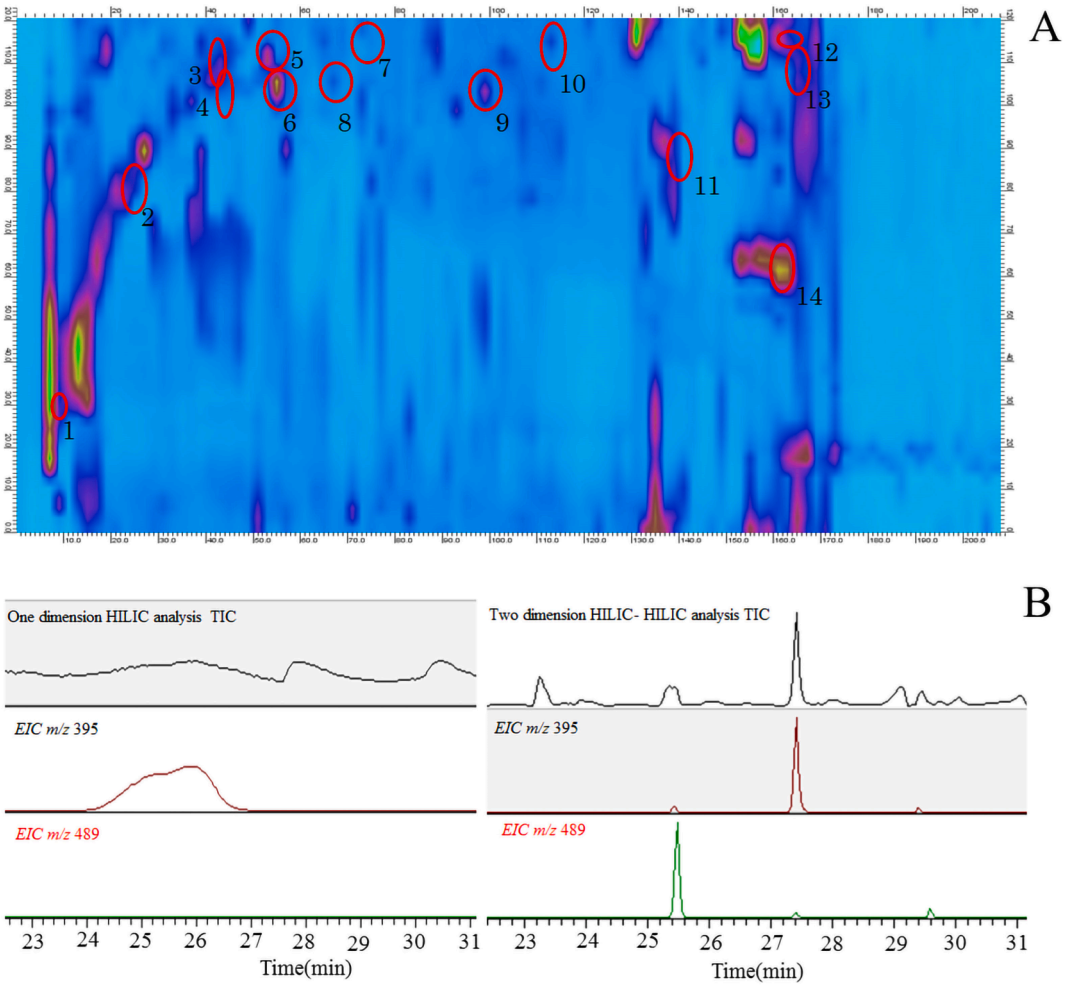

Fig. 3. (A) The separation of safflower sample on 2D-TIC contour plots by using the optimal online HILIC × HILIC-ESI/HRMS/MS^n system, (B) The separation comparison of 1D-HILIC and HILIC × HILIC in safflower.

Welch Materials). Water containing 0.2 μM ammonium formate (A) and acetonitrile (B) were used as mobile phases. The following segment gradient program with six different segments was applied: *i*) 0–55 min (0 min, 96% B; 0.25 min, 96% B; 1.7 min, 85% B; 1.75 min, 96% B, 2 min, 96% B), *ii*) 56–73 min (0 min, 93% B; 0.25 min, 93% B; 1.7 min, 85% B; 1.75 min, 93% B, 2 min, 93% B), *iii*) 74–91 min (0 min, 90% B; 0.25 min, 90% B; 1.7 min, 82% B; 1.75 min, 90% B, 2 min,90% B) , *iv*) 92–130 min (0 min, 90% B; 0.25 min, 90% B; 1.7 min, 80% B; 1.75 min, 90% B, 2 min, 90% B), *v*) 131–140 min (0 min, 85% B; 0.25 min, 85% B; 1.7 min, 75% B; 1.75 min, 85% B, 2 min, 85% B), *vi*) 141–170 min (0 min, 85% B; 0.25 min, 85% B; 1.7 min, 70% B; 1.75 min, 85% B, 2 min, 85% B). The other parameters were set as follows: DAD sampling rate, 50 Hz; detection wavelength, 281 nm; column temperature, 30 °C; injection volume, 3 μL; and modulation cycle, 2 min.

For the ESI/HRMS/MS^2 analyses, samples introduced from the flow splitter were analyzed in the positive ion mode. The MS parameters were employed as below: capillary temperature, 350 °C; spray voltage, 4 kV; capillary voltage, 35 V; and tube lens voltage, 120 V. Both auxiliary and sheath gases were nitrogen (N_2), set at flow rates of 8 and 10 arbitrary units, respectively. In the linear ion trap, the collision gas was high-purity helium (He).

A full scan event followed by two data-dependent acquisition (DDA) events were present in the scan cycle. Accurate mass data from *m/z* 100 to 1200 was recorded by the Orbitrap mass analyzer in the full scan event, and its resolution was set at 30,000 (FWHM as defined at *m/z* 400). In DDA events, MS^2 fragment data were acquired in the linear ion trap triggered by the top two intension ions from the full scan event. Collision-induced dissociation (CID) activation was optimized to a normalized collision energy of 35% with the isolation width set at *m/z* 2.0. The dynamic exclusion function was enabled for DDA events. The Orbitrap mass analyzer was weekly calibrated to maintain high mass accuracy using the calibration solution according to the manufacturer's guidelines.

Data analyses

Raw HRMS and MS^2 data were visualized and processed by the Xcalibur 2.1 software. The 2D contour plot was built using the LC Image LC × LC-HRMS Edition software (version 2.6, GC Image, LLC., Lincoln, NE, USA). The LC Image software was also used for 2D peaks recognition and location. Effective peak capacity, theoretical peak capacity, orthogonality, and practical peak capacity were computed as previously described (Filgueira et al., 2011; Qiao et al., 2014; Qiao et al., 2015).

Results and discussion

Establishment of the HILIC × HILIC system

Two offline HILIC-HILIC methods were carried out as previously reported to analyze polar components (Liu et al., 2009) and flavonoid O-glycosides (Yao et al., 2017) in the safflower, respectively. However, offline techniques are more time-consuming and may result in sample

Table 1
Characterization of polar constituents by HILIC × HILIC-LTQ-Orbitrap from safflower in positive ion mode.

Peak No.	Retention time 1st dim. (min)	Retention time 2nd dim. (sec)	Measured^{+} (m/z)	Error (ppm)	Molecular formula	(+) LC/ESI-MS^2 m/z (% base peak)	Identification	Ref.
1[S]	6	18	271.05933	−2.8	$C_{15}H_{10}O_5$		Apigenin	(Yang et al., 2016)
2	6	37.1	584.27661	2.0	$C_{34}H_{37}N_3O_6$	438.29,420.26,275.28	N_1,N_5,N_{10}-(Z)-tri-p-coumaroylspermidine	(Zhou et al., 2014)
3	10	41.8	584.27621	1.58	$C_{34}H_{37}N_3O_6$	438.34,420.33	N_1,N_5,N_{10}-(E)-tri-p-coumaroylspermidine	(Zhou et al., 2014)
4	14	32	584.27651	−4.6	$C_{34}H_{37}N_3O_6$	438.4,420.9	Safflospermidine A	(Zhou et al., 2014)
5	14	46	584.27635	−4.6	$C_{34}H_{37}N_3O6$	438.37,420.37	Safflospermidine B	(Zhou et al., 2014)
6	14	90.5	361.0917	−1.7	$C_{18}H_{16}O_8$		Rosmarinic acid	(Zhou et al., 2014)
7	16	60.3	373.11194(M + Na)	−3.8	$C_{20}H_{18}N_2O_4$	329.28,270.95,227.08	Serotobenine	(Sato et al., 2014)
8	16	116	439.12247	−2.81	$C_{20}H_{22}O_{11}$	395.30,353.26,292.31,204.07	Y-Glc-2C	(Yao et al., 2017)
9	20	76.6	409.1843(M + Na)	0.82	$C_{19}H_{30}O_8$	391.18,381.41,247.15,203.17,	Roseoside	(Zhou et al., 2014)
10	20	76	481.12955	−2.89	$C_{22}H_{24}O_{12}$	437.15,395.17	3,5,7,4′-tetrahydroxy-6-methoxyflavanonol-O-Glc	(Yao et al., 2017)
11	22	76	409.18417	0.98	$C_{19}H_{30}O_8$	390.48,365.31,289.16,202.95	Roseoside	(Yang et al., 2016)
12	22	76	289.07153	0.86	$C_{15}H_{12}O_6$	271.07,168.88,146.94	Eriodictiol	(Yang et al., 2016)
13	26	2.3	343.13742	−1.29	$C_{16}H_{22}O_8$	347.06,305.09,275.21,203.03,185.06	Methyl-3-(4-O-β-D-glucopyranosylphenyl) propionate or Bidenoside D	(Zhou et al., 2008)
14	26	90.5	395.13223(M + Na)	0.7	$C_{17}H_{24}O_9$	364.09,233.09,185.12	Methyl-3-(4-O-β-D-glucopyranosyl-3-methoxyphenyl) propionate	(Zhou et al., 2014)
15[S]	28	80	449.10783	−2.0	$C_{21}H_{20}O_{11}$	287.08	Quercitrin	
16	32	95	136.06177	0.3	C_5 H_5 N_5	135.87,118.17,108.08,	Adenine	(Zhou et al., 2014)
17	32	92.9	119.0355	1.6	$C_4H_6O_4$	91.05	Succinic acid	(Zhou et al., 2014)
18	38	78	385.14783	1.4	$C_{18}H_{24}O_9$	223.16,207.12,203.10	(-)-4-Hydroxybenzoic acid-4-O-[6́-O-(2 "- methylbutyryl)-β-D-glucopyranoside]	(Jiang et al., 2013)
19[S]	42	113	465.10275	1.0	$C_{21}H_{20}O_{12}$	446.23,303.08,279.27	Hyperoside	(Zhou et al., 2014)
20[S]	44	104	465.10159	1.2	$C_{21}H_{20}O_{12}$	447.32,303.07	Isoquercitrin	(Zhou et al., 2014)
21[S]	52	111	625.17444	1.9	$C_{28}H_{32}O_{16}$	479.15,317.06,301.98	6-Methoxykaempferol 3-O-Rutinoside	(Yang et al., 2016)
22	52	111	317.06516	2.7	$C_{16}H_{12}O_7$	302.12	5-Methoxyquercetin	(Yang et al., 2016)
23	54	100	311.1492	0.9	$C_{16}H_{22}O_6$	293.27,191.13	2Z-Decaene-4,6-diyn-1-O- -β-glucopyranoside	(Hong et al., 2015)
24	54	102	625.17847	0.2	$C_{28}H_{32}O_{16}$	479.15,317.06,301.98	Isorhamnetin methylpentosyl hexoside isomer	(Yang et al., 2016)
25[S]	54	104	595.16498	2.8	C_{27} $H_{30}O_{15}$	449.21,287.04	Kaempferol-3-O-rutinoside	(Yue et al., 2013)
26	54	102	1151.31848(2 M + H)	4.5	$C_{27}H_{29}NO_{13}$		Cartormin	(Yin & He, 2000)
27	54	102	317.0655	2.7	$C_{16}H_{12}O_7$	302.08	5-Methoxyquercetin isomer	(Yao et al., 2017)
28	54	104.5	449.10889	1.2	$C_{21}H_{20}O_{11}$	453.27,435.27,417.28,387.27	Kaempferol-3-O-β-D-glucoside	(Zhou et al., 2014)
29	56	78.9	615.17041	−0.4	$C_{30}H_{30}O_{14}$	597.37,571.31,501.15,451.20,289.18	Safflomin C	(Si et al., 2016)
30	56	88	595.16523	1.5	$C_{27}H_{30}O_{15}$	599.31,573.61,471.36,331.17	Saffloquinoside C isomer	(Zhou et al., 2014)
31	56	88	449.10907	1.2	$C_{21}H_{20}O_{11}$	453.27,435.27,417.28	Luteolin-7-O-β-D-glucopyranoside	(Zhou et al., 2014)
32	62	85	463.0871	−0.5	$C_{21}H_{18}O_{12}$	445.32, 287.10	Scutellarin	(Yang et al., 2016)
33	64	113.8	244.09352	0.9	$C_9H_{13}N_3O_5$	226.11,148.08	Cytidine	(Yao et al., 2016)
34	66	4	595.16547	−0.4	$C_{27}H_{30}O_{15}$	577.30,433.13	Saffloquinoside C	

(*continued on next page*)

Table 1 (*continued*)

Peak No.	Retention time 1st dim. (min)	2nd dim. (*sec*)	Measured^{+} (*m/z*)	Error (ppm)	Molecular formula	(+) LC/ESI-MS^2 *m/z* (% base peak)	Identification	Ref.
								(Zhou et al., 2014)
35[S]	66	104	465.10275	0.9	$C_{21}H_{20}O_{12}$	447.34,380.35,345.02,303.04	Quercimeritrin	(Zhou et al., 2014)
36	66	62.7	595.16553	−0.3	$C_{27}H_{30}O_{15}$	577.42,551.46,449.21,433.24,287.16	Safflor yellow A	(Yue et al., 2013)
37	66	104	487.17722	−3.9	$C_{22}H_{30}O_{12}$	469.41,420.38,403.18	(8Z)-decaene-4,6-diyn-1-ol-1-O-β-D-glucuronyl-(100–20)-β-Dglucopyranoside	(He et al., 2011)
38	70	4.6	284.09894	1.1	$C_{10}H_{13}N_5O_5$		Guanosine	(Fan et al., 2009)
39	70	48	633.1394(M + Na)	−5.0	$C_{27}H_{30}O_{16}$	615.40,487.32,347.19,337.1	6-MeO-Kae-O-Glc-Xyl	(Yang et al., 2016)
40	70	4.6	649.11884(M + K)	3.2	$C_{27}H_{30}O_{16}$	631.22,529.14,487.37,363.04	Kaempferol 3-O-β-sophoroside	(Kazuma et al., 2000)
41	70	116	491.11172	7.5	$C_{23}H_{22}O_{12}$	495.17,469.25,367.24,331.22	Luteolin-7-O-(6′′-O-acetyl)-β-D-glucoside	(Yang et al., 2016)
42	72	67	465.10263	1.3	$C_{21}H_{20}O_{12}$	447.19,363.20,345.08,303.01	Quercimeritrin isomer	(Zhou et al., 2014)
43	72	111.5	633.14636(M + Na)	3.1	$C_{27}H_{30}O_{16}$	631.19,621.27,605.36,473.50	Quercetin 3-O-rutinoside	(Kazuma et al., 2000)
44	72	4	611.15576	−8.0	$C_{27}H_{30}O_{16}$	465.25,303.04	Y-2Glc—CH_2 isomer	(Yang et al., 2016)
45	72	109	611.15717	−5.7	$C_{27}H_{30}O_{16}$	593.36,449.22,303.07	Y-2Glc—CH_2 isomer	(Yang et al., 2016)
46	74	78	611.15723	−5.6	$C_{27}H_{30}O_{16}$	567.22,435.29,391.19	Y-2Glc—CH_2	(Yang et al., 2016)
47[S]	76	67	611.15723	−5.6	$C_{27}H_{30}O_{16}$	593.41,567.49, 465.22, 303.02	rutin	(Yang et al., 2016)
48	76	13	697.1593	−2.5	$C_{30}H_{32}O_{19}$	679.48,653.37,535.30,287.06	Kae-3-O-diglucoside-Mal.	(Yao et al., 2017)
49	78	74	433.11292	−0.9	$C_{21}H_{20}O_{10}$	415.15,397.10,313.17,301.07	Saffochalconeside	(Hong et al., 2015)
50	80	58	633.1394(M + Na)	−1.4	$C_{27}H_{30}O_{16}$	615.32,487.16,331.19	Que-3,6 or 3,7-di-O-Xyl-GluA	(Yang et al., 2016)
51	82	25	713.15375	−3.1	$C_{30}H_{32}O_{20}$	551.33,303.13	6-OH-Kae-3,6 or 3,7-di-O-diglucoside-Mal.	(Yao et al., 2017)
52	84	4	611.15686	−6.2	$C_{27}H_{30}O_{16}$	465.27,303.09	Y-2Glc—CH_2 isomer	(Yang et al., 2016)
53	86	95	625.17596	−0.5	$C_{28}H_{32}O_{16}$	479.09,317.16	5,7,4′-trihydroxy-6-methoxy-flavonol-3-O-rutinoside	(Yao et al., 2017)
54	88	92	461.10342	9.0	$C_{22}H_{20}O_{11}$	439.24,397.22,235.11	Acacetin-7-O-β-D-glucuronide	(Yao et al., 2017)
55	90	16.2	123.04441	0.3	$C_7H_6O_2$	99.95,81.81	p-hydroxybenzaldehyde	(Yang et al., 2016)
56	92	78	451.1524	−2.0	$C_{21}H_{22}O_{11}$	433.23,304.17,289.16	Neocarthamin	(Hong et al., 2015)
57	92	20	697.15881	−3.2	$C_{30}H_{32}O_{19}$	535.26,287.05	6-OCH_3-Kae-3-O-GlC-Rha-Oxa	(Yang et al., 2016)
58[S]	98	102	627.15771	2.4	$C_{27}H_{30}O_{17}$	465.16,303.09	6-Hydroxykaempferol 3,6-diglucoside	(Zhou et al., 2014)
59	102	109.1	629.17358	2.2	$C_{27}H_{32}O_{17}$	611.41,403.17	Methylisosafflomin C	(Zhou et al., 2014)
60	106	18	576.16858	−4.4	$C_{27}H_{29}NO_{13}$		Cartormin isomer	(Yang et al., 2016)
61	116	76	595.16574	1.5	$C_{27}H_{30}O_{15}$	577.54,433.18,415.09,397.20,313.23,301.19,277.19	Saffloquinoside A	(Hong et al., 2015; Zhou et al., 2014)
62[S]	120	90	625.13992	3.2	$C_{27}H_{28}O_{17}$	606.50,463.03,449.24,340.34,311.33,287.17	6-hydroxyapigenin-6-O-β-D-glucoside-7-O-β-D-glucuronide	(Kazuma et al., 2000)
63[N]	130	111	409.13150	2.0	$C_{14}H_{26}O_{12}$	277.10,317.18	Propanetriol-Glu	
64[N]	130	72	409.13068	−5.5	$C_{14}H_{26}O_{12}$	277.10	Propanetriol-Glu isomer	
65	132	116	365.10678	−3.1	$C_{12}H_{22}O_{11}$	275.06,203.00,184.95	Sucrose or its isomers	(Kubica et al., 2012)
66[S]	136	90.5	773.21716	3.4	$C_{33}H_{40}O_{21}$	754.42,627.24,610.45,465.18,303.03	6-Hydroxykaempferol 3-Rutinoside−6-glucoside	(Zhou et al., 2008)
67[N]	136	104	409.13330	2.2	$C_{14}H_{26}O_{12}$	277.14,317.12,	Propanetriol-Glu isomer	
68	144	11	957.22687	−3.6	$C_{44}H_{44}O_{24}$	938.48,902.45,825.59,794.37	Precarthamin	(Yang et al., 2016)
69	144	9.2	911.22113	−4.2	$C_{43}H_{42}O_{22}$		Carthamin isomer	(Yang et al., 2016)
70	146	71	957.2264	−3.0	$C_{44}H_{44}O_{24}$		Precarthamin isomer	

(*continued on next page*)

Table 1 (*continued*)

Peak No.	Retention time 1st dim. (min)	2nd dim. (*sec*)	Measured^{+} (*m/z*)	Error (ppm)	Molecular formula	(+) LC/ESI-MS^2 *m/z* (% base peak)	Identification	Ref.
								(Yang et al., 2016)
71	150	11	911.22113	−4.3	$C_{43}H_{42}O_{22}$		Carthamin isomer	(Yang et al., 2016)
72	152	116.1	1045.281958	4.8	$C_{48}H_{52}O_{26}$	1027.55,868.64,788.42	Anhydrosafflor Yellow B isomer	(Yang et al., 2016)
73	154	39	415.10034	2.5	$C_{21}H_{18}O_9$	397.29, 367.23, 295.15	Saffloflavonesides A isomer	(Yang et al., 2016)
74 [N]	154	4	501.17966	−4.2	$C_{19}H_{32}O_{15}$	482.45,339.10,193.07	Quinic acid-Glu-Rha	(Yang et al., 2016)
75 [N]	156	88	501.17926	−5.8	$C_{19}H_{32}O_{15}$	482.32,339.21,285.09,193.06	Quinic acid- Glu-Rha isomer	(Yang et al., 2016)
76	156	18	541.17578	−4.9	$C_{19}H_{34}O_{16}$	409.21,317.12,277.22	Propanetriol-Glu-Xyl-Xyl	(Yang et al., 2016)
77[S]	158	13.9	613.1763	−5.3	$C_{27}H_{32}O_{16}$	594.36,577.07,549.51,451.20,433.22,331.06,317.27,301.07	Hydroxysafflor yellow A	(Yue et al., 2013)
78	158	16	415.1007	0.9	$C_{21}H_{18}O_9$	397.23,367.21,355.14	Saffloflavonesides A isomer	(Yang et al., 2016)
79	160	37	415.10129	3.9	$C_{21}H_{18}O_9$		Saffloflavonesides A	(Yang et al., 2016)
80	160	76	629.17035	−4.8	$C_{27}H_{32}O_{17}$	633.27, 531.40,489.19	3,5,6,7,4′-Pentahydroxyflavanonol-O-Glc-Glc	(Yao et al., 2017)
81	162	62.7	1045.281958	7.9	$C_{48}H_{52}O_{26}$	1027.44,1009.62,955.66,822.85,720.67	Anhydrosafflor yellow B	(Fan et al., 2009)
82	162	16.2	1045.281958	0.8	$C_{48}H_{52}O_{26}$	1026.60,883.44,721.28	Anhydrosafflor yellow B isomer	(Fan et al., 2009)
83[S]	162	111	789.21167	7.3	$C_{33}H_{40}O_{22}$		6-Hydroxykaempferol-3,6,7-triglucoside	(Kazuma et al., 2000)
84	162	65	629.19305	0.4	$C_{31}H_{32}O_{14}$	633.33,531.40,489.21	Methylsafflomin C or methylisosafflomin	(Yoon, 2008)
85[S]	164	109.1	803.20355	4.2	$C_{33}H_{38}O_{23}$	784.45,641.33,479.32,341.21,303.13	6-Hydroxyl kaempherol-3,6-O-diglucosyl-7-O-Glucuronic acid	(Kazuma et al., 2000)
86	164	16	1063.2925	−2.0	$C_{48}H_{54}O_{27}$	1045.50,1022.25,697.42	Safflomin B isomer	(Yue et al., 2013)
87	164	16	1063.2925	−1.9	$C_{48}H_{54}O_{27}$	1622.32,1467.74,833.92	Safflor yellow B	(Yang et al., 2016)
88	164	60	641.14673	−5.1	$C_{27}H_{28}O_{18}$	645.42,619.62	Quercetin-3-O-α-L-rhamnoside-7-O-β-D-glucuronide	(Yao et al., 2017)
89	166	76	629.18648	3.2	$C_{31}H_{32}O_{14}$		Methylisosafflomin C	(Yue et al., 2013)
90	166	85	1063.29028	−2.1	$C_{48}H_{54}O_{27}$	1039.21,907.82,578.38	Safflomin B	(Yao et al., 2017)
91	166	51	911.22113	−3.2	$C_{43}H_{42}O_{22}$		Carthamin	(Sato et al., 2003)
92	168	9	935.26355	−2.9	$C_{39}H_{50}O_{26}$		6-OH-Kae-3,6 or 3,7-di-O-Glc-Glc-Rha-Glc	(Yang et al., 2016)
93	168	116	309.12915	−4.1	$C_{16}H_{20}O_6$	291.16,273.16,225.07	(2E,8Z)-Decadiene-4,6-diyne-1-ol-1-O-β-D-glucopyranoside.	(He et al., 2011)

[S] , indicates the compound was confirmed by reference compounds. [N], indicates the compound was identified in safflower for the first time. Y, represents the quinochalcone C-glycoside skeletons with the elemental compositions of $C_{16}H_{12}O_6$.

loss. Therefore, an online 2D-LC strategy was considered and optimized in the current study. Since the main chemicals in safflower were polar ingredients, columns with HILIC mode were preferred for 2D separations. In HILIC, analytes exhibited similar retention behaviors to those of NPLC, and an RP solvent system can be used for separation, which is suitable for polar components analyses. Thus, after a series of optimizations including column types, mobile phases, gradient elution programs, and flow rates, good separation with evenly distributed peaks was finally achieved on an XBridge Amide column (150 mm × 4.6 mm, 3.5 μm, Waters), employed as the ^{1}D column (Fig. S1). It should be particularly noted that, in order to reduce the injection band broadening in ^{2}D separation, the long and narrow columns (e.g., 1 or 2.1 mm i.d.) were preferred as ^{1}D columns. In the current study, although the column with amide stationary phase was demonstrated to be the best choice for ^{1}D separation, a 4.6 mm i.d. column was the only amide option in this study, which was limited by our column resources. Therefore, to minimize injection volume in ^{2}D separation and also provide enough ^{1}D peak samplings, the ^{1}D flow should be operated under the suboptimal linear flow velocities, which was 0.08 mL/min in this study.

To achieve high orthogonality, the combination of HILIC and RPLC was considered first to configure the 2D-LC system. Three RP columns with different stationary phases, including Hypersil gold PFP (150 mm × 2.1 mm, 3 μm), Accucore aQ (50 mm × 4.6 mm, 2.6 μm) and Accucore Polar Premium (50 mm × 3.0 mm, 2.6 μm) were tested for the ^{2}D separation. The best combination was determined by evaluating the correlation coefficient (R^2) between the selected ^{1}D column and the tested ^{2}D columns. Results showed that the combinations of XBridge Amide with Hypersil gold PFP and Accucore Polar Premium provided similar low R^2 values as 0.03 and 0.01, respectively, being both suitable for ^{2}D separation according to the evaluation index. Thus, these two

combinations were applied to analyze the 14 references. Unfortunately, the severe solvent incompatible effect was observed under both column combinations, and each reference compound was splitted into two independent peaks with different 2D RTs (Fig. 2A and 2B). The peaks width in the second dimension were about 80 s in Fig. 2A and 2B. The weaker elution solvent (high acetonitrile ratio) in the ^{1}D HILIC analysis is the stronger one in the ^{2}D RP analysis, which might have led to the loss of separation resolution and efficiency.

To solve the solvent incompatible effect problem, an online dilution module was integrated into the 2D-LC system. Briefly, another LC pump was connected to the outlet of the ^{1}D HILIC column to introduce a continuous water phase for the organic phase dilution from ^{1}D fractions (Cao et al., 2017). References with retention time (RT) lower than 110 min in the ^{1}D analysis were well separated without peak splitting (Fig. 2C). However, for the references with larger polarities (^{1}D RT > 110 min), peak splitting was still observed despite the peaks width in the second dimension had reduced to about 65 s. Due to the large polarities of these compounds in safflower, it is difficult to build an online HILIC × RP system with high efficiency and resolution, even using an online dilution strategy. Hence, we considered a combination of HILIC × HILIC to reconfigure the 2D-LC system. According to the literature, the HILIC × HILIC employing stationary phases with different functional groups can also offer different selectivity and possible high orthogonality (Wang et al., 2008).

Thus, different HILIC columns were tested for the ^{2}D separation. Samples were separated on short broad-bore columns and eluted at a relatively high flow rate. Therefore, we finally applied a HILIC column named Ultimate amide column (50 mm × 4.6 mm, 5 μm) for the ^{2}D separation in this study. A high flow rate of 3 mL/min was employed to reduce the large volume influence of sample solvent and maintained the system pressure in a reasonable range. The cycle duration should guarantee that the ^{1}D eluent will not exceed the ^{2}D 200-μL sample loops. Thus, the valve switched every 2 min, and 160 μL (80 μL/min × 2 min) fractions eluted from the ^{1}D separation was re-injected to the ^{2}D column for each modulation cycle.

Segment gradient programs were optimized with six different segments as described above. A high flow rate of 3 mL/min was also selected to provide efficient and fast ^{2}D separation. Finally, the safflower sample was well separated on the 2D contour plots under the optimized parameters in 170 min without any visible peak splitting (Fig. 3A), which reduced the possibility of false identification of polar components.

HILIC × HILIC system evaluation

The established HILIC × HILIC system was evaluated by separating a real safflower sample. On the 2D-TIC contour plot, 213 peaks were recognized by the LC Image software (blob filter settings: minimum volume = 0, minimum area = 3, minimum peak = 5, relative values). The effective gradient time for ^{1}D was 175 min and for ^{2}D was 2 min. The average 4σ peak widths were 2 min and 0.117 min in ^{1}D and ^{2}D chromatograms, respectively. Hence, the theoretical peak capacities were 87 and 17.1 for ^{1}D and ^{2}D analysis, respectively. Then, the effective and theoretical peak capacity was calculated as 817 and 1487 for the optimized HILIC × HILIC system, indicating a much higher separation capability compared to 1D-LC analyses (Li and Schmitz, 2015; Wang et al., 2008).

According to reported equations (Filgueira et al., 2011; Li et al, 2009), the practical peak capacity and orthogonality were evaluated by dividing the separation space into 14 × 14 rectangular bins, which was close to P_{max} (2 1 3) and superimposed with the data points (Fig. S2). Our results showed that about 62.75% of the separation space was covered by bins containing data points. Finally, the practical peak capacity and orthogonality were calculated as 932 and 88.27%, respectively (Filgueira et al., 2011; Qiao et al., 2015).

Separation and characterization of flavonoids and alkaloids in safflower

The developed HILIC × HILIC system was used to analyze the flavonoids and alkaloids in safflower. On the 2D-TIC contour plot, the compounds were separated and detected as blobs. In contrast with conventional 1D-LC analyses, the established 2D-LC system exhibited a remarkable separation power. For example, the EIC *m/z* 395 in safflower got sufficient sampling of three times in the ^{2}D separation with high resolution and excellent peak shape (Fig. 3B). Besides, some undetectable components in 1D-HILIC, such as *m/z* 489, were successfully detected with high sensitivity by using the established HILIC × HILIC system, indicating its high resolving power and feasibility (Fig. 3).

By analyzing their accurate mass and fragmentation data, and comparing with reference standards, 93 constituents were identified or tentatively identified, including 5 flavonoids, 24 flavonoid C-glycosides, 46 flavonoid O-glycosides and 10 alkaloids (summarized in Table 1). Among them, 5 new constituents were found in safflower for the first time. Herein, the structural elucidation of several representative compounds and potentially new ones were discussed as examples.

Compound 2 gave the accurate mass at *m/z* 584.27661 $[M + H]^+$ and its formula was calculated to be $C_{34}H_{37}N_3O_6$. In the MS^2 spectra, ions at *m/z* 438 and *m/z* 420 were observed resulting from the loss of $C_9H_6O_2$ and $C_9H_{10}O_2N$, respectively. Further, these data were further compared with the literature (Zhao et al., 2009) and compound 2 was finally identified as N_1,N_5,N_{10}-(Z)-tri-p-coumaroylspermidine. Its MS^2 spectra and proposed fragmentation are shown in Fig. 4A.

Compounds 61 and 25 presented the same $[M + H]^+$ ion at *m/z* 595.16547. Their formula was calculated as $C_{27}H_{30}O_{15}$. However, their MS^2 spectra different. Compound 25 showed fragments at *m/z* 576, 449, and 287. The characteristic neutral loss of 162 Da and 146 Da indicated it was a bioside (Fig. 4B and 4D). The MS^2 spectra of compound 61, showed ions at *m/z* 577, 433, 415, 397, 385, 313, 301, and 277. The calculated elimination of 162 Da indicated glucose (glc) disaccharide moiety. According to the literature (Li et al., 2013; Lu et al., 2019), the element composition and fragmentation behaviors of compound 61 were consistent with that of saffloquinoside A, reported from *Pueraria lobata*. Therefore, compound 61 was tentatively characterized as saffloquinoside A.

Compound 65 showed an adduct ion $[M + Na]^+$ at *m/z* 365.10684 and a deprotonated molecular ion $[M-H]^-$ at *m/z* 341.10712 with a calculated empirical molecular formula of $C_{12}H_{22}O_{11}$. In its MS^2 spectra, the neutral loss of 18, 60, and 162 Da were observed with the production of fragment ions at *m/z* 347, 305, 203 in the positive ion mode, and *m/z* 323, 281, 179 in the negative ion mode, indicating the loss of H_2O and glucose (Fig. 4C and 4E). By comparing with literature (Kubica, et al., 2012), the calculated molecular formula and MS^2 data were consistent with sucrose or its isomers. Thus, compound 65 was tentatively identified as sucrose or its isomers ($C_{12}H_{22}O_{11}$).

In the current study, we tentatively characterized 5 new constituents in safflower for the first time. To reduce false chemical identifications, a negative ion mode was also applied to provide the supplementary data for verification. Compound 63 was presented the $[M + Na]^+$ ion at *m/z* 409.13290 and $[M-H]^-$ ion at *m/z* 385.13284 with the calculated element composition as $C_{14}H_{26}O_{12}$. This formula was consistent with Propanetriol-α-L-arabinofuranosyl (1 → 4)-β-D-glucopyranoside, a safflower compound recorded in the TCM Database@Taiwan (http://tcm.cmu.edu.tw/zh-tw/chemical.php?compoundid = 37322). For compound 63, the MS^2 spectra showed fragment ions at *m/z* 317 and 277 in positive ion mode, and *m/z* 253 in negative ion mode, indicating the loss of 92 Da and pentoses (Fig. 5A and 5C). Additionally, in the MS^3 spectra of *m/z* 277, a loss of 92 Da and glucose was observed (Fig. 5B). Comparing these results with the chemical structure of Propanetriol-α-L-arabinofuranosyl (1 → 4)-β-D-glucopyranoside, we deduced that the loss of 92 Da was produced by the elimination of the propanetriol group. Besides, loss of H_2O and CO were observed, indicating a polyhydric aglycone. However, the glycogen linkage can not be deduced only by

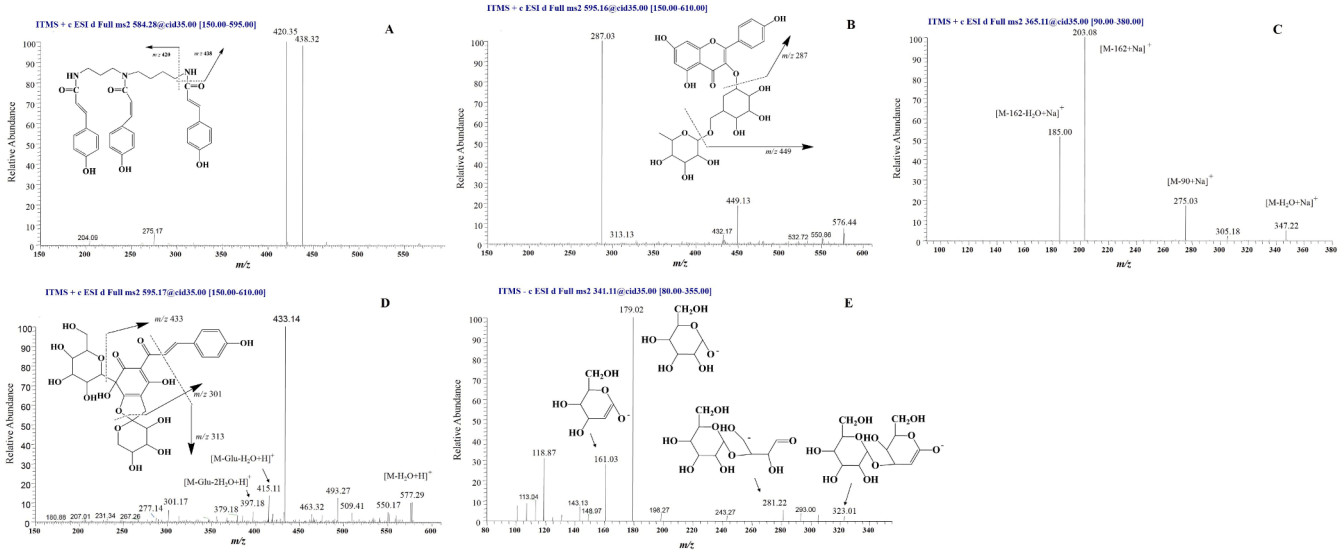

Fig. 4. The MS/MS spectra and proposed fragmentation pathway for compound 2 (A), and the MS/MS spectra and proposed fragmentation pathway for compound 25 (B) and 61 (D), and compound 65 under positive ion mode (C) and negative ion mode (E).

mass spectrometry. Therefore, compound 63 was tentatively identified as Propanetriol-Glu. The MS data of compounds 64 and 67 were similar to compound 63 and they were both tentatively identified as isomers.

Compound 74 gave accurate mass at *m/z* 501.18088 in the positive ion mode and *m/z* 499.16415 in the negative ion mode, and was determined as be $C_{19}H_{32}O_{15}$ with errors lower than 3 ppm. Its MS^2 spectra in the negative ion mode showed ions at *m/z* 481, 353, 191 and 173 (Fig. 6), indicating $[M\text{-}H\text{-}H_2O]^-$, $[M\text{-}H\text{-}rha]^-$, $[M\text{-}H\text{-}rha\text{-}glu]^-$ and $[M\text{-}H\text{-}rha\text{-}glu\text{-}H_2O]^-$ ions. Typical fragment ions at *m/z* 191 and 173 were identified as quinic acid according to the literature (Clifford & Nikolai Kuhnert, 2005; Lin & Harnly, 2007; Deborah et al., 2007). Thus, aglycone was assigned to quinic acid. In the positive ion mode MS^2 spectra, the observed losses of 18 and 64 Da were matched the fracture behavior reported before (Cheng et al., 2008; Yuan et al., 2015). In the MS^3 spectra, the neutral loss of H_2O and CO indicated that the aglycone was polyhydric. Therefore, compound 74 was putatively characterized as

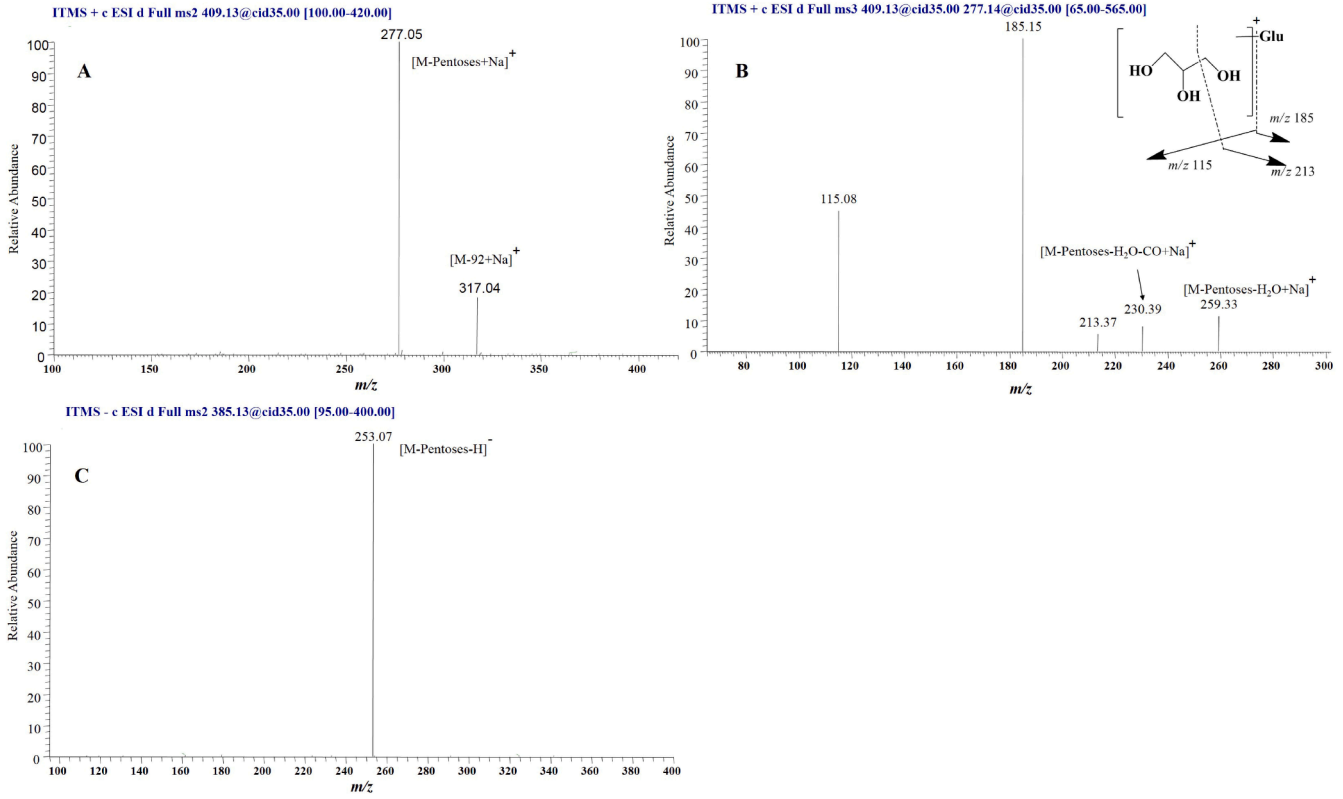

Fig. 5. The MS/MS/MS spectra and proposed fragmentation pattern for compound 63 under positive ion mode (A, B) and negative ion mode (C).

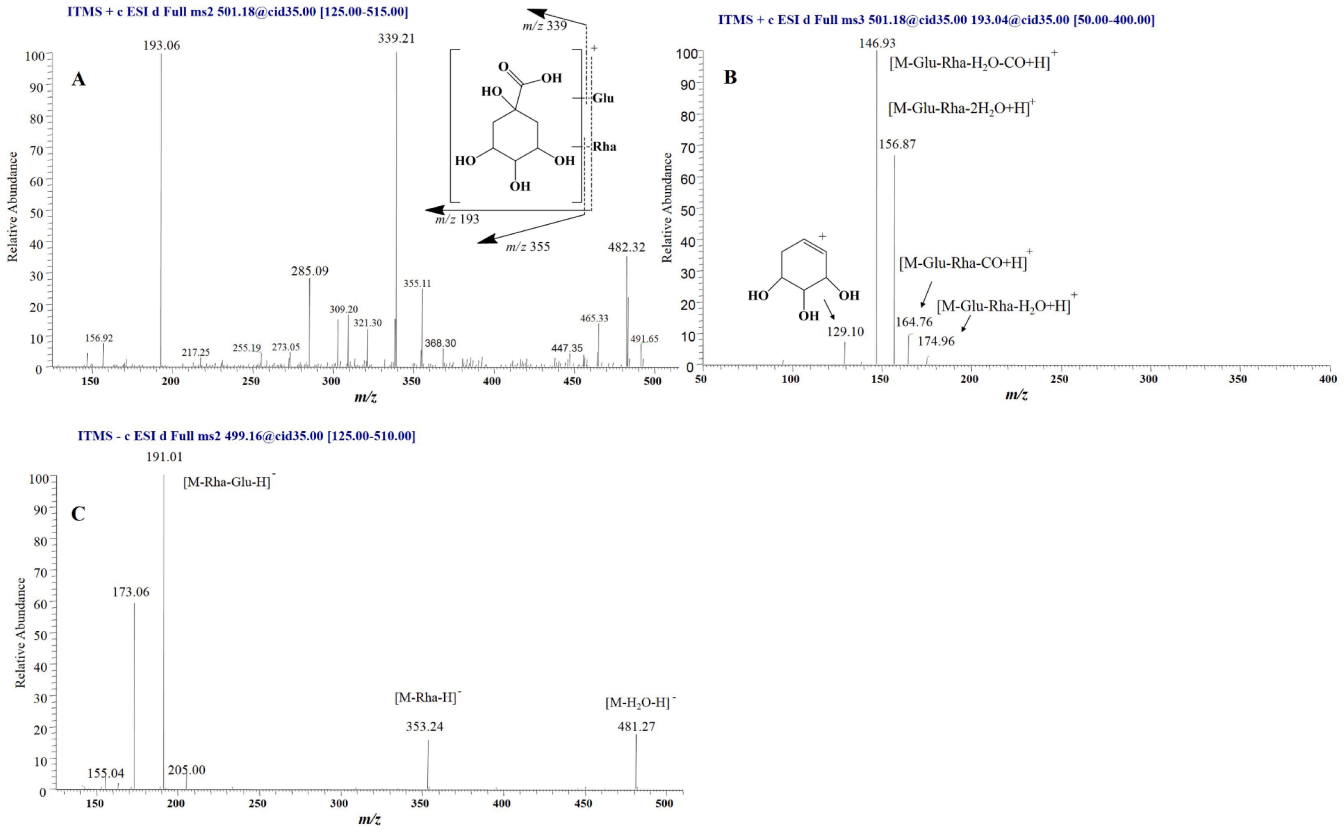

Fig. 6. The MS^n spectra and proposed fragmentation pattern for compound 74 under positive ion mode (A, B) and negative ion mode (C).

quinic acid-Glu-Rha. Compound 75 showed the same fragmentation behavior of 74, and was then characterized as an isomer.

Conclusions

In the current study, an online HILIC × HILIC-DAD-ESI/HRMS/MS^n system was optimized and applied to analyze the flavonoids and alkaloids of safflower. The mobile phase incompatibility problem was solved by the combination of HILIC and HILIC with high orthogonality. Under optimal conditions, the orthogonality was as high as 88.27%, leading to the detection of 231 peaks on the 2D-TIC contour plot. Among them, 93 compounds were clearly or tentatively identified, including 5 potentially new ones, using the complementary structural information acquired by both negative and positive ion modes. Overall, the established HILIC × HILIC-DAD-ESI/HRMS/MS^n system demonstrated its efficiency and powerful to analyze compounds in complex herbal extracts.

Declaration of Competing Interest

The authors declare that they have no known competing financial interests or personal relationships that could have appeared to influence the work reported in this paper.

Acknowledgements

This work was supported by Research Committee of the University of Macau (grant number MYRG2018-00239-ICMS), Macau Science and Technology Development Fund (grant number 147/2019/A3), Guangxi Innovation-driven Development Special Foundation Project (grant number GuiKe AA18118049), and Sichuan Science and Technology Planning Project (grant number 2020YFS0370).

Appendix A. Supplementary data

Supplementary data to this article can be found online at https://doi.org/10.1016/j.fochx.2021.100143.

References.

Cao, J., Chen, Z., Zhu, Y., Li, Y., Guo, C., Gao, K., … Wen, A. (2014). Huangqi-Honghua combination and its main components ameliorate cerebral infarction with Qi deficiency and blood stasis syndrome by antioxidant action in rats. *J Ethnopharmacol, 155*(2), 1053–1060. https://doi.org/10.1016/j.jep.2014.05.061

Cao, J. L., Wang, S. S., Hu, H., He, C. W., Wan, J. B., Su, H. X., & Li, P. (2017). Online comprehensive two-dimensional hydrophilic interaction chromatographyxreversed-phase liquid chromatography coupled with hybrid linear ion trap Orbitrap mass spectrometry for the analysis of phenolic acids in Salvia miltiorrhiza. *J Chromatogr A*. https://doi.org/10.1016/j.chroma.2017.09.041

Cao, J. L., Wei, J. C., Hu, Y. J., He, C. W., Chen, M. W., Wan, J. B., & Li, P. (2016). Qualitative and quantitative characterization of phenolic and diterpenoid constituents in Danshen (Salvia miltiorrhiza) by comprehensive two-dimensional liquid chromatography coupled with hybrid linear ion trap Orbitrap mass. *J Chromatogr A, 1427*, 79–89. https://doi.org/10.1016/j.chroma.2015.11.078

Cheng, L., Zhang, M., Zhang, P., Song, Z., Ma, Z., & Qu, H. (2008). Silver complexation and tandem mass spectrometry for differentiation of triterpenoid saponins from the roots of Pulsatilla chinensis (Bunge) Regel. *Rapid Commun Mass Spectrom, 22*(23), 3783–3790. https://doi.org/10.1002/rcm.v22:2310.1002/rcm.3801

Dai, Y., Verpoorte, R., & Choi, Y. H. (2014). Natural deep eutectic solvents providing enhanced stability of natural colorants from safflower (Carthamus tinctorius). *Food Chem, 159*, 116–121. https://doi.org/10.1016/j.foodchem.2014.02.155

Deborah H. Markowicz Bastos , L. A. S., Rodrigo R. Catharino , Alexandra C., & H. F. Sawaya , I. B. S. C., Patrícia O. Carvalho , Marcos N. Eberlin. (2007). Phenolic Antioxidants Identified by ESI-MS from Yerba Maté (Ilex paraguariensis) and Green Tea (Camelia sinensis) Extracts. *Molecules, 12*, 423-432. https://www.mdpi.com/1420-3049/12/3/423.

Delshad, E., Yousefi, M., Sasannezhad, P., Rakhshandeh, H., & Ayati, Z. (2018). Medical uses of Carthamus tinctorius L. (Safflower): A comprehensive review from Traditional Medicine to Modern Medicine. *Electron Physician, 10*(4), 6672–6681. https://doi.org/10.19082/6672

Donato, P., Cacciola, F., Sommella, E., Fanali, C., Dugo, L., Dacha, M., & Mondello, L. (2011). Online comprehensive RPLC x RPLC with mass spectrometry detection for the analysis of proteome samples. *Anal Chem, 83*(7), 2485–2491. https://doi.org/10.1021/ac102656b

Fan, L., Zhao, H.-Y., Xu, M., Zhou, L., Guo, H., Han, J., … Guo, D. A. (2009). Qualitative evaluation and quantitative determination of 10 major active components in Carthamus tinctorius L. by high-performance liquid chromatography coupled with diode array detector. *J Chromatogr A, 1216*(11), 2063–2070. https://doi.org/10.1016/j.chroma.2008.03.046

Filgueira, M. R., Huang, Y., Witt, K., Castells, C., & Carr, P. W. (2011). Improving peak capacity in fast online comprehensive two-dimensional liquid chromatography with post-first-dimension flow splitting. *Anal Chem, 83*(24), 9531–9539. https://doi.org/10.1021/ac202317m

He, J., Shen, Y., Jiang, J. S., Yang, Y. N., Feng, Z. M., Zhang, P. C., … Hou, Q. (2011). New polyacetylene glucosides from the florets of Carthamus tinctorius and their weak anti-inflammatory activities. *Carbohydr Res, 346*(13), 1903–1908. https://doi.org/10.1016/j.carres.2011.06.015

He, Y., Wan, H., Du, Y., Bie, X., Zhao, T., Fu, W., & Xing, P. (2012). Protective effect of Danhong injection on cerebral ischemia-reperfusion injury in rats. *J Ethnopharmacol, 144*(2), 387–394. https://doi.org/10.1016/j.jep.2012.09.025

Hong, B., Wang, Z., Xu, T., Li, C., & Li, W. (2015). Matrix solid-phase dispersion extraction followed by high performance liquid chromatography-diode array detection and ultra performance liquid chromatography-quadrupole-time of flight-mass spectrometer method for the determination of the main compounds from Carthamus tinctorius L. (Hong-hua). *J Pharm Biomed Anal, 107*, 464–472. https://doi.org/10.1016/j.jpba.2015.01.040

Jiang, J. S., Chen, Z., Yang, Y. N., Feng, Z. M., & Zhang, P. C. (2013). Two new glycosides from the florets of Carthamus tinctorius. *J Asian Nat Prod Res, 15*(5), 427–432. https://doi.org/10.1080/10286020.2013.780046

Kazuma, K., Takahashi, T., Sato, K., Takeuchi, H., Matsumoto, T., & Okuno, T. (2000). Quinochalcones and flavonoids from fresh florets in different cultivars of Carthamus tinctorius L. *Biosci Biotechnol Biochem, 64*(8), 1588–1599. https://doi.org/10.1271/bbb.64.1588

Li, D., Duck, R., & Schmitz, O. J. (2014). The advantage of mixed-mode separation in the first dimension of comprehensive two-dimensional liquid-chromatography. *J Chromatogr A, 1358*, 128–135. https://doi.org/10.1016/j.chroma.2014.06.086

Li, D., Jakob, C., & Schmitz, O. (2015). Practical considerations in comprehensive two-dimensional liquid chromatography systems (LCxLC) with reversed-phases in both dimensions. *Anal Bioanal Chem, 407*(1), 153–167. https://doi.org/10.1007/s00216-014-8179-8

Li, D., & Schmitz, O. J. (2015). Comprehensive two-dimensional liquid chromatography tandem diode array detector (DAD) and accurate mass QTOF-MS for the analysis of flavonoids and iridoid glycosides in Hedyotis diffusa. *Anal Bioanal Chem, 407*(1), 231–240. https://doi.org/10.1007/s00216-014-8057-4

Li, L., Yang, Y., Hou, X., Gu, D., Ba, H., Abdulla, R., … Aisa, H. A. (2013). Bioassay-guided separation and purification of water-soluble antioxidants from Carthamus tinctorius L. by combination of chromatographic techniques. *Separation and Purification Technology, 104*, 200–207. https://doi.org/10.1016/j.seppur.2012.11.027

Liang, Z., Li, K., Wang, X., Ke, Y., Jin, Y., & Liang, X. (2012). Combination of off-line two-dimensional hydrophilic interaction liquid chromatography for polar fraction and two-dimensional hydrophilic interaction liquid chromatographyxreversed-phase liquid chromatography for medium-polar fraction in a traditional Chinese medicine. *J Chromatogr A, 1224*, 61–69. https://doi.org/10.1016/j.chroma.2011.12.046

Lin, L. Z., & Harnly, J. M. (2007). A Screening Method for the Identification of Glycosylated Flavonoids and Other Phenolic Compounds Using a Standard Analytical Approach for All Plant Materials. *J. Agric. Food Chem., 55*, 1084–1096. https://doi.org/10.1021/jf062431s

Liu, Y., Guo, Z., Feng, J., Xue, X., Zhang, F., Xu, Q., & Liang, X. (2009). Development of orthogonal two-dimensional hydrophilic interaction chromatography systems with the introduction of novel stationary phases. *J Sep Sci, 32*(17), 2871–2876. https://doi.org/10.1002/jssc.200900086

Clifford, Micheal N., & Nikolai Kuhnert, S. K. (2005). Discriminating between the Six Isomers of Dicaffeoylquinic Acid by LC-MSn. *J. Agric. Food Chem., 53*(10), 3821–3832. https://doi.org/10.1021/jf050046h

Lu, J. X., Zhang, C. X., Hu, Y., Zhang, M. H, Wang, Y. N., Qian, Y. X., … Guo, D. A. (2019). Application of multiple chemical and biological approaches for quality assessment of Carthamus tinctorius L. (safflower) by determining both the primary and secondary metabolites. *Phytomedicine, 58*, 152826. https://doi.org/10.1016/j.phymed.2019.152826

Paola Dugo, O. F., Luppino, Rosario, Dugo, Giovanni, & Mondello, Luigi (2004). Comprehensive Two-Dimensional Normal-Phase (Adsorption)-Reversed-Phase Liquid Chromatography. *Analytical Chemistry, 76*(9), 2525–2530. https://doi.org/10.1021/ac0352981

Qiao, X., Song, W., Ji, S., Li, Y.-jiao., Wang, Y., Li, R., … Ye, M. (2014). Separation and detection of minor constituents in herbal medicines using a combination of heart-cutting and comprehensive two-dimensional liquid chromatography. *J Chromatogr A, 1362*, 157–167. https://doi.org/10.1016/j.chroma.2014.08.038

Qiao, X., Song, W., Ji, S., Wang, Q., Guo, D. A., & Ye, M. (2015). Separation and characterization of phenolic compounds and triterpenoid saponins in licorice (Glycyrrhiza uralensis) using mobile phase-dependent reversed-phasexreversed-phase comprehensive two-dimensional liquid chromatography coupled with mass spectrometry. *J Chromatogr A, 1402*, 36–45. https://doi.org/10.1016/j.chroma.2015.05.006

Sato, H., Kawagishi, H., Nishimura, T., Yoneyama, S., Yoshimoto, Y., Sakamura, S., … Matsumoto, T. (2014). Serotobenine, a Novel Phenolic Amide from Safflower Seeds (Carthamus tinctoriusL.). *Agricultural and Biological Chemistry, 49*(10), 2969–2974. https://doi.org/10.1080/00021369.1985.10867182

Sato, K., Sugimoto, N., Ohta, M., Yamazaki, T., Maitani, T., & Tanamoto, K. (2003). Structure determination of minor red pigment in carthamus red colorant isolated by preparative LC/MS. *Food Addit Contam, 20*(11), 1015–1022. https://doi.org/10.1080/02652030310001615177

Si, W., Yang, W., Guo, D., Wu, J., Zhang, J., Qiu, S., … Wu, W. (2016). Selective ion monitoring of quinochalcone C-glycoside markers for the simultaneous identification of Carthamus tinctorius L. in eleven Chinese patent medicines by UHPLC/QTOF MS. *J Pharm Biomed Anal, 117*, 510–521. https://doi.org/10.1016/j.jpba.2015.09.025

Sommella, E., Ismail, O. H., Pagano, F., Pepe, G., Ostacolo, C., Mazzoccanti, G., & Campiglia, P. (2017). Development of an improved online comprehensive hydrophilic interaction chromatography x reversed-phase ultra-high-pressure liquid chromatography platform for complex multiclass polyphenolic sample analysis. *J Sep Sci, 40*(10), 2188–2197. https://doi.org/10.1002/jssc.201700134

Uliyanchenko, E., Cools, P. J., van der Wal, S., & Schoenmakers, P. J. (2012). Comprehensive two-dimensional ultrahigh-pressure liquid chromatography for separations of polymers. *Anal Chem, 84*(18), 7802–7809. https://doi.org/10.1021/ac3011582

Villa, C., Costa, J., Oliveira, M. B., & Mafra, I. (2017). Novel quantitative real-time PCR approach to determine safflower (Carthamus tinctorius) adulteration in saffron (Crocus sativus). *Food Chem, 229*, 680–687. https://doi.org/10.1016/j.foodchem.2017.02.136

Wang, S. S., Xu, H. Y., Ma, Y., Wang, X. G., Shi, Y., Huang, B., … Yang, H. J. (2015). Characterization and rapid identification of chemical constituents of NaoXinTong capsules by UHPLC-linear ion trap/Orbitrap mass spectrometry. *J Pharm Biomed Anal, 111*, 104–118. https://doi.org/10.1016/j.jpba.2015.01.020

Wang, Y., Lu, X., & Xu, G. (2008). Development of a comprehensive two-dimensional hydrophilic interaction chromatography/quadrupole time-of-flight mass spectrometry system and its application in separation and identification of saponins from Quillaja saponaria. *J Chromatogr A, 1181*(1–2), 51–59. https://doi.org/10.1016/j.chroma.2007.12.034

Yang, W., Si, W., Zhang, J., Yang, M., Pan, H., Wu, J., … Guo, D. (2016). Selective and comprehensive characterization of the quinochalcone C-glycoside homologs in Carthamus tinctorius L. by offline comprehensive two-dimensional liquid chromatography/LTQ-Orbitrap MS coupled with versatile data mining strategies†. *RSC Advances, 6*(1), 495–506. https://doi.org/10.1039/C5RA23744K

Li, X., Stoll, D. R., & Carr, P. W. (2009). Equation for Peak Capacity Estimation in Two-Dimensional Liquid Chromatography. *Anal. Chem, 81*(2), 845–850. https://doi.org/10.1021/ac801772u

Yao, C.-liang., Yang, W.-zhi., Si, W., Shen, Y., Zhang, N.-xia., Chen, H.-li., … Guo, D.-an. (2017). An enhanced targeted identification strategy for the selective identification of flavonoid O-glycosides from Carthamus tinctorius by integrating offline two-dimensional liquid chromatography/linear ion-trap-Orbitrap mass spectrometry, high-resolution diagnostic product ions/neutral loss filtering and liquid chromatography-solid phase extraction-nuclear magnetic resonance. *J Chromatogr A, 1491*, 87–97. https://doi.org/10.1016/j.chroma.2017.02.041

Yao, D., Wang, Z., Miao, L., & Wang, L. (2016). Effects of extracts and isolated compounds from safflower on some index of promoting blood circulation and regulating menstruation. *J Ethnopharmacol, 191*, 264–272. https://doi.org/10.1016/j.jep.2016.06.009

Yin, H. B., & He, Z. S. (2000). A novel semi-quinone chalcone sharing a pyrrole ring C-glycoside from Carthamus tinctorius. *Tetrahedron Letters, 41*(12), 1955–1958. https://doi.org/10.1016/S0040-4039(00)00100-3

Yoon, H. R. (2008). Radical-Scavenging Activities of Four Quinochalcones of Safflower. *Journal of the Korean Society for Applied Biological Chemistry, 51*(4), 346–348. https://doi.org/10.3839/jksabc10.3839/jksabc.2008.061

Yuan, L., Zhang, Z., Hou, Z., Yang, B., Li, A., Guo, X., … Li, Y. (2015). Rapid classification and identification of complex chemical compositions in traditional Chinese medicine based on UPLC-Q-TOF/MS coupled with data processing techniques using the KuDieZi injection as an example. *Analytical Methods, 7*(12), 5210–5217. https://doi.org/10.1039/C4AY03103B

Yue, S., Tang, Y., Li, S., & Duan, J. A. (2013). Chemical and biological properties of quinochalcone C-glycosides from the florets of Carthamus tinctorius. *Molecules, 18*(12), 15220–15254. https://doi.org/10.3390/molecules181215220

Zhao, G., Gai, Y., Chu, W. J., Qin, G. W., & Guo, L. H. (2009). A novel compound N(1), N(5)-(Z)-N(10)-(E)-tri-p-coumaroylspermidine isolated from Carthamus tinctorius L. and acting by serotonin transporter inhibition. *Eur Neuropsychopharmacol, 19*(10), 749–758. https://doi.org/10.1016/j.euroneuro.2009.06.009

Zhou, X., Tang, L., Xu, Y., Zhou, G., & Wang, Z. (2014). Towards a better understanding of medicinal uses of Carthamus tinctorius L. in traditional Chinese medicine: A phytochemical and pharmacological review. *J Ethnopharmacol, 151*(1), 27–43. https://doi.org/10.1016/j.jep.2013.10.050

Zhou, Y. Z., Chen, H., Qiao, L., Xu, N., Cao, J. Q., & Pei, Y. H. (2008). Two new compounds from Carthamus tinctorius. *J Asian Nat Prod Res, 10*(5–6), 429–433. https://doi.org/10.1080/10286020801892425

Xiao, J., Capanoglu, E., Jassbi, A. R., & Miron, A. (2016). Advance on the Flavonoid C-glycosides and Health Benefits. *Crit Rev Food Sci Nutr, 56*(Suppl 1), S29–S45. https://doi.org/10.1080/10408398.2015.1067595

Zhang, L. L., Tian, K., Tang, Z. H., Chen, X. J., Bian, Z. X., Wang, Y. T., & Lu, J. J. (2016). Phytochemistry and Pharmacology of Carthamus tinctorius L. *Am J Chin Med, 44*(2), 197–226. https://doi.org/10.1142/S0192415X16500130

Kubica, P., Kot-Wasik, A., Wasik, A., Namiesnik, J., & Landowski, P. (2012). Modern approach for determination of lactulose, mannitol and sucrose in human urine using HPLC-MS/MS for the studies of intestinal and upper digestive tract permeability. *J Chromatogr B Analyt Technol Biomed Life Sci, 907*, 34–40. https://doi.org/10.1016/j.jchromb.2012.08.031